

Pseudo-Plastic Behaviour of Single-Crystals of Cu-Base Memory Alloys

V. Prieb and H. Steckmann*

1st Memory Alloys GmbH Techn. Büro Berlin, Sembritzkistr. 9A, 12169 Berlin, Germany

** 1st Memory Alloys GmbH Hauptstrasse 24, 61279 Grävenwiesbach 2, Germany*

Abstract: The hysteretic behaviour of Cu-Al-X single-crystals (with X = Zn, Mn, Ni) deforming in the martensitic state is investigated. The tension-compression partial and complete deformation cycles show no dependence of the hysteresis on the temperature, a zero-stress diagonal, at which the yields and recovery begin. "Return point memory" and degradation of the hysteresis with decreasing deformation amplitude have been found at the pseudo-plastic behaviour. Thermodynamic transformation parameters and the hysteresis interior of complete and partial thermal-induced, stress-free transformations are received by calorimetry.

1. Introduction

Phenomenological models describe the thermoelastic equilibrium of the austenite-martensite two-phase system with the hysteresis during thermoelastic martensitic transformations in shape memory alloys as a balance of three transformation driving forces: chemical, non-chemical and dissipative ones [1].

Müller's theory [2] takes into consideration no storage of the elastic energy (no thermoelasticity) and identifies this elastic energy (the coherency energy of phase interfaces) with the dissipated energy. This shape of the pseudoelastic hysteresis loops was found by Fu's unique experiment on Cu-Al-Zn single-crystals. It is also proposed in this theory as well as in other theories based on Landau's phenomenological consideration the temperature dependence of the pseudo-plastic hysteresis. The pseudo-plastic hysteresis and its peculiarities were never experimentally investigated in detail because it requires to combine tension-compression stress in one run.

Parameters of the pseudo-plastic partial and major hysteresis loops from detailed tension-compression tests as well as thermodynamic parameters of the thermal hysteresis with the help of calorimetry are determined in this work.

2. Experimental

2.1 Alloys and procedures

The shape memory alloys (Tab. 1) were melted from components with the purity 99.99% in a graphite crucible under argon atmosphere. Single-crystals were grown by a modified Bridgman method. The single crystals were homogenised at 1125 K for 24 h and cut along the crystal axis into the deformation test samples with a gauge volume $38 \times 2.5 \times 2$ (mm³) and wide grip parts. Discs $\varnothing 5$ mm and 0.5 mm thickness for the calorimetric measurements were cut normal to the crystal axis.

Tension-compression tests were carried out with an "in-situ" apparatus which allows to vary the sample temperature, to observe the sample surface on an optical microscope, or to carry out measurements of the electrical resistance during the tension-compression tests. The single-crystal orientation was determined by the two-surface analysis. Calorimetric measurements were carried out in a DSC-7 calorimeter of the Perkin-Elmer PC - series. The electrical resistance was measured with the "four-points" method at a stabilised current 4 A.

Table 1 Composition (at%), axis orientation, and transformation temperatures (K) of the samples

No.	Cu	Al	Zn	Mn	Ni	$[hkl]_{B2}$	M_s	M_f	A_s	A_f
1	68.8	15.2	16.0	--	--	100	289.5	286.4	290.7	293.0
2	68.6	20.7	--	10.7	--	110	300.0	287.0	308.0	322.0
3	70.6	24.7	--	--	4.7	110	382.6	376.1	384.1	389.8

All samples were standard heat treated as follows: annealing at 1125 K for 0.2 h, then quenching into oil at 425 K for 0.5 h, and then quenching into water at the room temperature.

2.2 Results

2.2.1 Hysteresis of thermal-induced, stress-free transformation

Transformation temperatures of the investigated single-crystals determined by calorimetry at the scanning rate 0.015 K/s are given in the Table 1. These temperature were obtained by the extrapolation of linear parts of the hysteresis loops $z(T)$ (Fig. 1 a) from $z = 1/2$ to $z = 0$ (M_s, A_f) and to $z = 1$ (M_f, A_s). The transformation temperatures and the hysteresis loop shape determined by resistometry (Fig. 1 b) agree with the calorimetric ones. Transformation temperatures measured during partial cycles $M'_s(z)$ (heating following the scheme $A_f > T_{i-1} > T_i > T_{i+1} > A_s$, and cooling all the time up to the same temperature $T < M_f$, where i is a cycle number) and $A'_s(z)$ (cooling under the scheme $M_f < T_{i-1} < T_i < T_{i+1} < M_s$ and heating up to the temperature $T > A_f$) build two straight lines which are not parallel with each other in the case of the asymmetrical hysteresis loop (Fig. 2 a, b). Hysteresis loops in their ideal shape consist in two triangles with equal squares on the left of the diagonal $M'_s(z)$ and on the right of the diagonal $A'_s(z)$. On Cu-Al-Mn single crystals there is a wide interval ($A'_s(z) - M'_s(z)$) (Fig. 1 a) which is very small on Cu-Al-Zn and Cu-Al-Ni single-crystals.

The measured and calculated transformation parameters are presented in the Table 2. The hysteresis of thermal-induced, stress-free transformation is described by the following parameters:

- equilibrium temperature bracketed by the $M'_s(z)$ and $A'_s(z)$ temperatures extrapolated to $z = 0$:

$$T_0 = \frac{M'_s(0) + A'_s(0)}{2} \text{ (will be later discussed);}$$

- hysteresis width at $z = 1/2$: $\Delta T = \frac{(A_f + A_s) - (M_s + M_f)}{2}$;

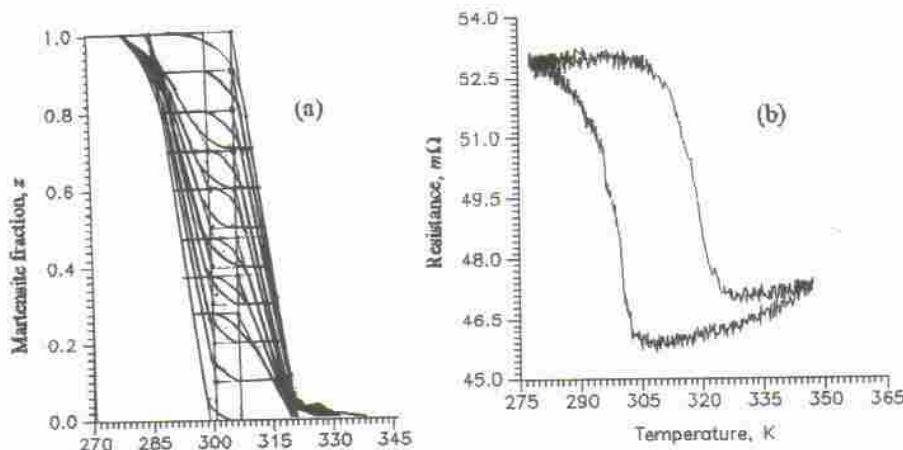


Fig. 1 Hysteresis loops by calorimetry (a) and resistometry (b). Sample 2.

- measured heat for the forward q^{AM} and reverse q^{MA} transformation;

$$\Delta s = \frac{q^{AM} + |q^{MA}|}{2T_0};$$

- "thermoelasticity" coefficient in an energy representation: $k_T = \frac{1}{2} \frac{dT}{dz} \Delta s$ or for the ideal

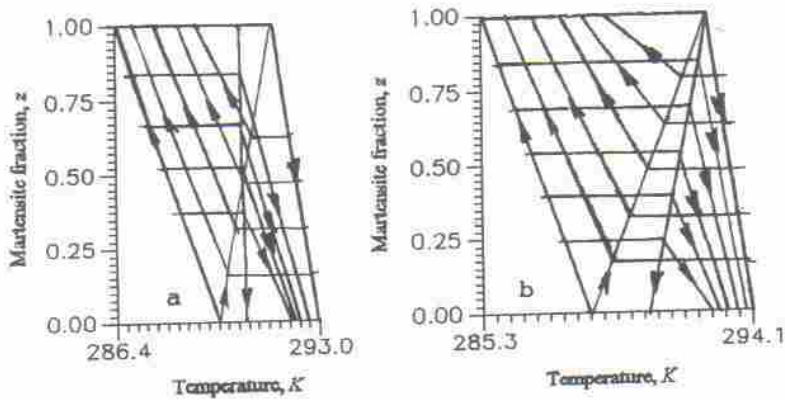


Fig. 2 Ideal hysteresis loops obtained at the rate 0.015 K/s (a) and 0.065 K/s (b). Sample 1.

hysteresis loops $k_T^{AM} \approx \frac{1}{2}(M_s - M_f)\Delta s$ for the full forward and $k_T^{MA} \approx \frac{1}{2}(A_f - A_s)\Delta s$ for the full reverse transformation;

- dissipated energy during the full cycle $w_D^T = \Delta T \cdot \Delta s$.

Table 2 Thermodynamic data from the calorimetry

No.	T_0, K	$\Delta T, K$	$q^{AM} / q^{MA}, \frac{J}{kg}$	$\Delta s, \frac{J}{kg \cdot K}$	$k_T^{AM} / k_T^{MA}, \frac{J}{kg}$	$w_D^T, \frac{J}{kg}$
1	289.8	3.9	6400/-6600	22.4	34.7/ 25.8	87.4
2	304.0	21.5	6600/-6800	22.0	143.0/154.0	473.0
3	383.6	7.6	7400/-8500	20.7	67.3/ 59.0	157.3

2.2.2 Pseudo-plastic hysteresis

Tension-compression tests of the samples in the martensitic state ($T < M_f$) show the hysteresis between the tension ($\sigma > 0$) and compression branches of the deformation diagrams (Fig. 3 a-c).

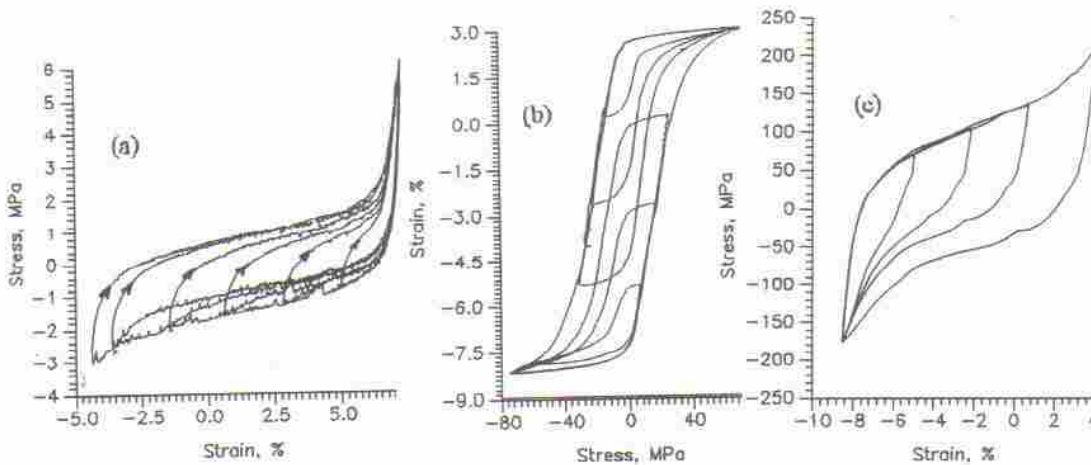


Fig. 3 Pseudo-plastic hysteresis and its interior on the sample 1 (a), 2 (b - the ferromagnetic kind of the axes representation), and 3 (c)

General features of the hysteresis are the following:

- a symmetric shape relative to the strain-axis which can be ideally presented as a parallelogram consisting in two triangles on the tension and compression stress-sides of the diagram (Fig. 3 a, b) or an internal parallelogram (the permanent hysteresis) and two triangles (Fig. 3 c);
- independence of the hysteresis parameters on the temperature;
- similarity of the pseudo-plastic (ferroelastic) hysteresis (Fig. 3 b, 5 a) to the ferromagnetic hysteresis;

The interior of the hysteresis by the partial cycling can be generalised as follows:

- internal elasticity at the returning back from the tension or compression loading;
- internal tension and compression yields;
- existence of a diagonal lying close to the strain-axis (zero-stress) which is built by the change points from the elasticity to the yields;
- congruence of the internal hysteresis loops and the major one;

A pseudo-plastic hysteresis loop is described by the following parameters:

- hysteresis width $\Delta\sigma$ (stress amplitude between the tension and compression yields);
- hysteresis length $\Delta\varepsilon$ (strain amplitude between two elastic branches);
- strengthening coefficient in the energy representation $k_\sigma = \frac{1}{\rho} \frac{d\sigma}{d\varepsilon} \approx \frac{\Delta\sigma}{\rho\Delta\varepsilon}$, where ρ is the alloy density (the last equation is true for the ideal hysteresis shape);

- dissipated energy during a complete tension-compression cycle $w_D^\sigma = \frac{\Delta\sigma \cdot \Delta\varepsilon}{\rho}$ (calculated from the square involved inside the hysteresis loop). All these parameters for the investigated alloys are listed in the Table 3.

Dependence of the electrical resistance on the strain (Fig. 4) measured during the stress-induced martensitic transformation $A \rightarrow M^+$ (pseudo-elastic deformation - $T > A_f$), the rearrangement of the martensite variants $M^- \rightarrow M^+$ (pseudo-plastic deformation $T < M_f$), or the both processes together $(A + M^\pm) \rightarrow M^+$ ($M_s > T > M_f$) is linear in all cases, but with a different proportionality coefficient (M^- and M^+ are here the single martensite domains obtained at the compression and tension stress correspondingly). The proportionality coefficient increases at a large strain value. This strain value corresponds to the points where the experimental hysteresis loop deviates from its ideal shape (Fig. 3). This points towards the change in the deformation mechanism from the rearrangement of martensite variants to the change inside of the martensite, as it was also shown by X-ray investigations [3].

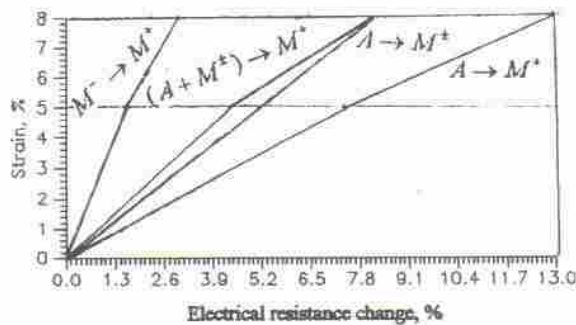


Fig. 4 Strain dependence of the resistance. Sample 2.

Table 3 Parameters of the pseudo-plastic hysteresis

No.	$\Delta\varepsilon$	$\Delta\sigma, MPa$	$k_\sigma, \frac{kJ}{kg}$	$w_D^\sigma, \frac{J}{kg}$
1	0.150	3.4	2.8	63.8
2	0.106	40.0	47.1	530.0
3	0.110	155.0(30)*	142.1	2131.3(412.5)*

*the permanent hysteresis is shown in brackets

Partial features of the major and internal hysteresis loops noticed by these deviations from the ideal shape are the following:

- internal pseudo-elasticity appearing as the inelastic deformation recovery during the tension or compression elastic unloading;
- congruence of the internal and major hysteresis loops is broken for the small deformation at the edges of the major hysteresis loop (Fig. 3), or inside it (Fig. 5 a, b).
- "return point memory" which consists of the closing of all the internal trajectories in the return points, from which these gone out (Fig. 5 a, b), on the nearest external hysteresis loop, eventually on the major one and never cross themselves.

All these effects are caused by the change of the strengthening coefficient. It is no more constant near to an elastic branch and increases asymptotically to the elastic modulus of the martensite with the decrease of the strain amplitude (Fig. 3 c, 5). Internal elasticity branches play the role of a boundary condition for internal loops. If the deformation amplitude of an internal loop is small, the whole internal trajectory has a strengthening coefficient different from the one of the major hysteresis loop and the internal loop is no more congruent with each other. It can be well seen on the Fig. 5 a, b with a spiral-like decreasing of the deformation amplitude of internal hysteresis loops. On the limit ($\varepsilon \rightarrow 0$) the hysteresis loop degrades to a straight line with the slope being equal to the elastic modulus of the martensite G . This limiting behaviour can be represented by a dependence of the slope of the second hysteresis loop diagonal (the line between the maximal magnitudes of the tension and compression stress inside a loop) on the

$$\text{strain: } k_{\sigma} \cdot \rho = \lim_{\Delta \varepsilon \rightarrow 0} \frac{\Delta \sigma_{\text{max}}^{\text{t-c}}(\varepsilon)}{\Delta \varepsilon} = G$$

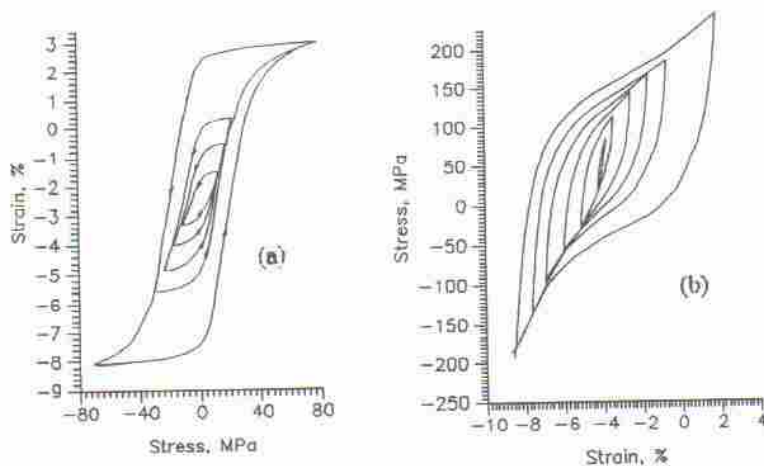


Fig. 5 Degradation of the ferroelastic hysteresis by the decreasing strain. Sample 2 (a) and 3 (b).

3. Discussion

Peculiarities of the pseudo-plastic hysteresis show that the equilibrium line has no slope relation with the external variable axis in absence of the phase transformation in the symmetrical (lattice parameter difference) and/or thermodynamic (entropy difference) sense. It, also, follows from Müller's theory considering the coherent nucleation of two phases with different lattice parameters. The whole pseudo-plastic hysteresis can be connected with the dissipation of the elastic energy arising from the martensite variant interaction during their rearrangement and described by parabolic dependence on the strain: $w_D = k_{\sigma}^0 + k_{\sigma} \varepsilon^2$, where $k_{\sigma}^0 \varepsilon$ is the permanent hysteresis which is absence on the samples 1 and 2.

The hysteresis interior of the stress-free transformation shows both kinds of the elastic energy appearance and its dissipation. The different slope of both equilibrium lines $M'_i(z)$ and $A'_i(z)$ can be interpreted as a different role of the nucleation for the forward and reverse transformation. The hysteresis of the stress-free transformation consists in two symmetrical contribution for the forward and reverse transformations:

$$w_D^{AM} = \frac{1}{2} \left[\frac{dM'_i(z)}{dz} - \frac{dA'_i(z)}{dz} \right] z \cdot \Delta s \cdot z = \left\{ [M'_i(1) - M'_i(0)] + [A'_i - A_i] \right\} \Delta s \cdot z^2 = w_D^{MA}$$

and the asymmetrical contribution for the forward transformation:

$$w_{D,as}^{AM} = \frac{1}{2} \left[\frac{dM'_i(z)}{dz} - \frac{dA'_i(z)}{dz} \right] z \cdot \Delta s \cdot z = \frac{1}{2} [(M_s - M_f) - (A_f - A_s)] \Delta s \cdot z^2. \text{ The whole dissipated energy is equal to their sum: } w_D^T = 2(k_T^{MA} + k_T^M)z^2, \text{ where } k_T^M = \frac{dM'_i(z)}{dz}.$$

The dissipative driving force is derived from the dissipated energy::

$$g_D^{AM} = (k_T^{MA} + k_T^M)z + (k_T^{MA} - k_T^M)z = (k_T^s + k_T^{as})z \text{ and } w_D^{MA} = (k_T^{MA} + k_T^M)z = k_T^s z.$$

The phase fraction dependence of the dissipative driving force connected with the martensite crystal interaction was shown for an symmetrical hysteresis loop by X-ray investigation on *NiTi*-polycrystals [4]. Two dissipative contributions for the stress-free (an asymmetrical hysteresis loop) and for the stress-induced (a symmetrical hysteresis loop) transformation, in agreement with our results, were found by internal friction investigation on the *Cu-Zn-Al*-polycrystals in the work [1]. The dissipated energy and stored elastic energy dependence has the same form as follows from these and our works. It means that namely the stored elastic energy (or part of it) dissipates. For the pseudo-plastic hysteresis the whole stored elastic energy dissipates, as it is shown here.

For the thermal hysteresis we can not conclude about the elastic energy storage, because it proposes a shift of the A_i -temperature in respect to the A_f -one, but the dissipation during the reverse transformation shifts the A_f temperature too. Therefore, it is not clear - whether the whole elastic energy dissipates by the auto-catalytic nucleation of martensite crystals and their self-accommodation, or a part of this energy is saved and causes the slope change of the equilibrium line. The elastic energy storage plays probably an important role on edges of non-ideal hysteresis loop, as it was shown on the *Mn-Cu* single-crystals [5] and by investigation of the strain dependence of the electrical resistance for the pseudo-plastic hysteresis.

Acknowledgements. Dr V. PrieB thanks the Federal Ministry for Education and Science of Germany and the Technical University Berlin for the financial and material support as well as Prof. I. Müller and Prof. Yu.I. Paskal for the inspiration of this work.

References

- [1] Gotthard R., Stoiber J., Bidaux J.-E., Proc. of the Int. Symposium SMM-94, Beijing, China, Sept. 25-28, ed. by Chu Younsi and Tu Hailing, Beijing, 1994, p.p. 309-313.
- [2] S. Fu, Y. Huo and I. Müller. Acta Mechanica 99 (1993) 1-19.
- [3] V. PrieB. J. de Physique IV, suppl. no. 11, 1 (1991) C4-317 - C4-322..
- [4] Paskal Yu. I. and Monasevich L. A., Phys. Met. Metall. 52 (1981) 95 - 99.
- [5] PrieB V. and Steckmann H., in these proceedings.